Three-Phase Displacement Theory: An Improved Description of Relative Permeabilities

Ruben Juanes, SPE, Stanford U.; and **Tad W. Patzek,** SPE, U. of California, Berkeley

Summary

In this paper, we revisit the displacement theory of three-phase flow and provide conditions for a relative permeability model to be physical anywhere in the saturation triangle. When capillarity is ignored, most relative permeability functions used today yield regions in the saturation space where the system of equations is locally elliptic, instead of hyperbolic. We are of the opinion that this behavior is not physical, and we identify necessary conditions that relative permeabilities must obey to preserve strict hyperbolicity. These conditions are in agreement with experimental observations and pore-scale physics.

We also present a general analytical solution to the Riemann problem (constant initial and injected states) for three-phase flow, when the system satisfies certain physical conditions that are natural extensions of the two-phase flow case. We describe the characteristic waves that may arise, concluding that only nine combinations of rarefactions, shocks, and rarefaction-shocks are possible. Some of these wave combinations may have been overlooked but can potentially be important in certain recovery processes.

The analytical developments presented here will be useful in the planning and interpretation of three-phase displacement experiments, in the formulation of consistent relative permeability models, and in the implementation of streamline simulators.

Introduction

Three immiscible fluids—water, oil, and gas—may flow in many processes of great practical importance: in primary production below bubblepoint and with movable water; in waterfloods, man-made and natural; in immiscible CO_2 floods; in steamfloods; in some gas condensate reservoirs; in gravity drainage of gas caps with oil and water; in WAG processes; and in contaminant intrusions into the shallow subsurface, just to name a few.

Relative permeabilities to water, oil, and gas are perhaps the most important rock/fluid descriptors in reservoir engineering. Currently, these permeabilities are routinely backed out from the theories of transient, high-rate displacements of inert and incompressible fluids that flow in short cores subjected to very high pressure gradients. More recently, the time evolution of area-averaged fluid saturations was measured with a CT scanner and, with several assumptions,[1] used to estimate the respective relative permeabilities in gravity drainage. Superior precision of the latter approach allowed the determination of relative permeabilities as low as 10^{-6}.

When the fractional-flow approach is used, flow of three immiscible incompressible fluids is described by a pressure equation and a 2×2 system of saturation equations.[2] It was long believed (at least in the Western literature) that, in the absence of capillarity, the system of equations would be hyperbolic for any relative permeability functions. This is far from being the case and, in fact, loss of hyperbolicity occurs for most relative permeability models used today. In this paper, we argue that such a behavior is not physically based, and we show how to overcome this deficiency. To do so, we adopt an opposite viewpoint to that of the existing literature: strict hyperbolicity of the system is assumed, and the implications on the functional form of the relative permeabilities are analyzed.

There is a theory behind each quantitative experiment. Not only does any theory reduce and abstract experience, but it also overreaches it by extra assumptions made for definiteness. Theory, in its turn, predicts the results of some specific experiments. The body of theory furnishes the concepts and formulæ by which experiment can be interpreted as being in accord or discord with it. Experiment, indeed, is a necessary adjunct to a physical theory, but it is an adjunct, not the master.[3] In other words, the relative permeability models are only as good as theories behind the displacement experiments from which these models have been obtained. If the theory is flawed, so are the relative permeabilities.

Mathematical Model

Governing Equations. We outline the mathematical formulation of multiphase flow in porous media under the following assumptions:

1. 1D flow.
2. Immiscible flow.
3. Incompressible fluids.
4. Homogeneous rigid porous medium.
5. Multiphase-flow extension of Darcy's law.
6. Negligible gravitational effects.
7. Negligible capillary pressure effects.

A detailed derivation of the governing equations can be found elsewhere.[2,4]

Assumption 2 prevents mass transfer between phases, and, therefore, one can identify components with phases. The 1D mass-conservation equation for the α phase is, in the absence of source terms,

$$\partial_t(m_\alpha) + \partial_x(F_\alpha) = 0, \quad (1)$$

where m_α = the mass density, F_α = the mass flux of the α-phase, and $\partial_t(\cdot)$, $\partial_x(\cdot)$ denote partial derivatives with respect to time and space, respectively. For three-phase flow, the system consists of aqueous, vapor, and liquid phases, corresponding to water (w), gas (g), and oil (o) components, respectively. The mass density of each phase is the mass per unit bulk volume of porous medium:

$$m_\alpha = \rho_\alpha S_\alpha \phi, \quad (2)$$

where ρ_α = the density of the α phase, S_α = the saturation, and ϕ = the porosity. Assumptions 3 and 4 make the phase densities and the porosity constant. Using the usual multiphase-flow extension of Darcy's law[5] (Assumption 5):

$$F_\alpha = -k\frac{k_{r\alpha}}{\mu_\alpha}\rho_\alpha(\partial_x p_\alpha + \rho_\alpha g \partial_x z), \quad (3)$$

where k = the absolute permeability, $k_{r\alpha}$ = the relative permeability, μ_α = the dynamic viscosity, and p_α = the pressure of the α phase. Relative permeabilities are assumed to be functions of phase saturations. The gravitational acceleration has absolute value g and points in the negative direction of the z-axis. We define the relative mobility of the α phase as

$$\lambda_\alpha := \frac{k_{r\alpha}}{\mu_\alpha}. \quad (4)$$

This paper (SPE 88973) was revised for publication from paper SPE 77539, presented at the 2002 SPE Annual Technical Conference and Exhibition, San Antonio, Texas, 29 September–2 October. Original manuscript received for review 9 January 2003. Revised manuscript received 30 May 2004. Manuscript peer approved 17 May 2004.

Neglecting gravitational and capillarity effects (Assumptions 6 and 7) the mass-conservation equation for the α phase is:

$$\partial_t S_\alpha + \partial_x \left(-\frac{1}{\phi} k\lambda_\alpha \partial_x p \right) = 0, \quad \ldots\ldots (5)$$

where p = the pressure, now common to all phases. Because the fluids fill up the pore volume, their saturations add up to one:

$$\sum_{\alpha=1}^{n} S_\alpha \equiv 1. \quad \ldots\ldots (6)$$

Adding the conservation equations for all phases and using the saturation constraint 6, we get the "pressure equation":

$$\partial_x \left(-\frac{1}{\phi} k\lambda_T \partial_x p \right) = 0, \quad \ldots\ldots (7)$$

where $\lambda T = \sum_{\alpha=1}^{n} \lambda\alpha$ is the total mobility. Eq. 7 dictates that the total velocity, defined as

$$v_T := -\frac{1}{\phi} k\lambda_T \partial_x p, \quad \ldots\ldots (8)$$

is at most a function of time. We now define the phase velocity

$$v_\alpha := \frac{\lambda_\alpha}{\lambda_T} v_T, \quad \ldots\ldots (9)$$

and the fractional flow for the α phase

$$f_\alpha := \frac{v_\alpha}{v_T} = \frac{\lambda_\alpha}{\lambda_T}. \quad \ldots\ldots (10)$$

With the definitions above, the three-phase flow system is governed by a 2×2 system of conservation laws,

$$\partial_t \begin{pmatrix} S_w \\ S_g \end{pmatrix} + v_T \partial_x \begin{pmatrix} f_w \\ f_g \end{pmatrix} = \begin{pmatrix} 0 \\ 0 \end{pmatrix}, \quad \ldots\ldots (11)$$

and the algebraic constraint $S_o = 1 - S_w - S_g$. The solution is restricted to lie in the saturation triangle

$$T := \{(S_w, S_g) : S_w \geq 0, \quad S_g \geq 0, \quad S_w + S_g \leq 1\}. \quad \ldots\ldots (12)$$

The saturation triangle is usually represented as a ternary diagram **(Fig. 1),** in which the pair S_w,S_g corresponds to the triple S_w,S_g,S_o, where $S_o \equiv 1 - S_w - S_g$.

Riemann Problem. Eq. 11 can be written in vector notation defining the vector of unknowns $\mathbf{u} = [u,v]^t = [S_w, S_g]^t$, and the flux vector $\mathbf{f} = [f,g]^t = [f_w, f_g]^t$. The Riemann problem for three-phase flow consists in finding a self-similar (usually weak) solution to the 2×2 system

$$\partial_t \mathbf{u} + v_T \partial_x \mathbf{f} = 0, \quad -\infty < x < \infty, t > 0, \quad \ldots\ldots (13)$$

with initial condition

$$\mathbf{u}(x,0) = \begin{cases} \mathbf{u}_l & \text{if } x < 0, \\ \mathbf{u}_r & \text{if } x > 0. \end{cases} \quad \ldots\ldots (14)$$

Unrealistic as it may seem (unbounded domain and piecewise constant initial data with a single discontinuity), the solution to the Riemann problem is extremely valuable for practical applications. Many laboratory experiments reproduce in fact the conditions of the Riemann problem: the medium has initially homogeneous saturations, and the proportion of injected fluids is held constant during the experiment. The solution to the Riemann problem also gives information about the structure of the system of equations and can be used as the building block for problems with more complex initial conditions (as in the Godunov method[6,7] or the front-tracking method[8]).

The property of self-similarity has been termed "stretching principle"[9] or "coherence condition"[10,11] in the petroleum engineering literature. It means that the solution at different times "can be obtained from one another by a similarity transformation."[12] We seek a solution of the form

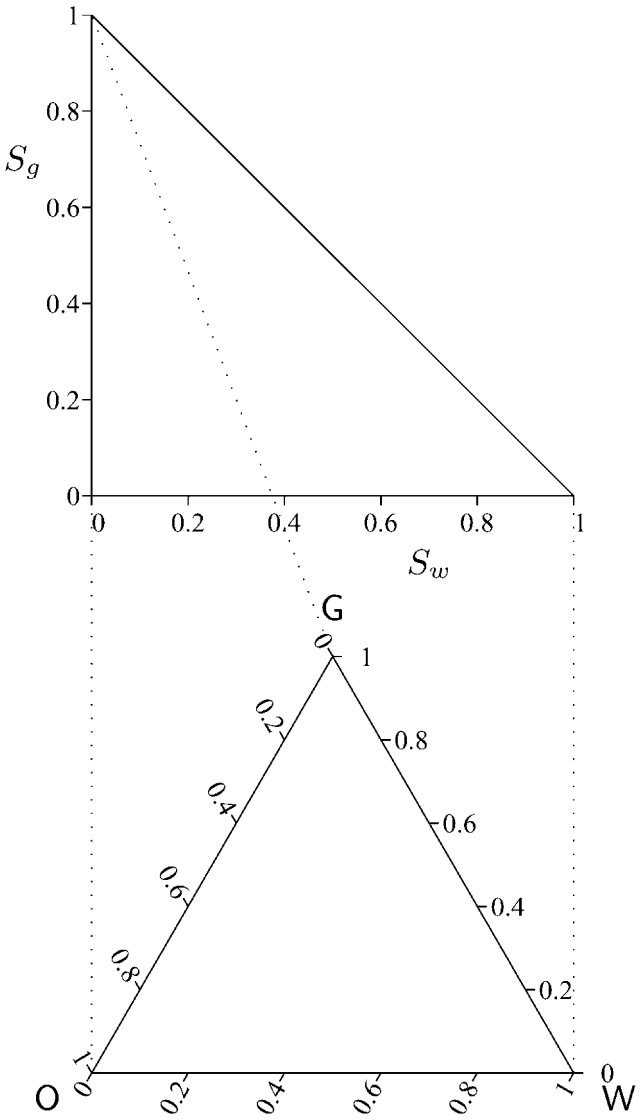

Fig. 1—Saturation triangle (top) and ternary diagram (bottom).

$$\mathbf{u}(x,t) = \mathbf{U}(\zeta). \quad \ldots\ldots (15)$$

In our case, the similarity variable ζ is

$$\zeta := \frac{x}{\int_0^t v_T(\tau) d\tau}. \quad \ldots\ldots (16)$$

Using Eqs. 15 and 16 in Eq. 13, the self-similar solution satisfies the system of ordinary differential equations

$$[\mathbf{A}(\mathbf{U}) - \zeta\mathbf{I}]\mathbf{U}' = 0, \quad -\infty < \zeta < \infty, \quad \ldots\ldots (17)$$

together with the boundary conditions

$$\mathbf{U}(-\infty) = \mathbf{u}_l, \quad \mathbf{U}(\infty) = \mathbf{u}_r, \quad \ldots\ldots (18)$$

where $\mathbf{A}(\mathbf{U})$ = the Jacobian matrix of the system; that is,

$$\mathbf{A}(\mathbf{U}) := D_{\mathbf{U}}\mathbf{f} = \begin{bmatrix} f_{,u}(\mathbf{U}) & f_{,v}(\mathbf{U}) \\ g_{,u}(\mathbf{U}) & g_{,v}(\mathbf{U}) \end{bmatrix}, \quad \ldots\ldots (19)$$

and $\mathbf{1}$ = the 2×2 identity matrix. Subscripts after a comma in Eq. 19 denote differentiation (*e.g.* $f_{,u} \equiv \partial_u f$).

Eqs. 17 and 18 define in fact an eigenvalue problem, where ζ is an eigenvalue, and $\mathbf{U}' = d\mathbf{U}/d\zeta$ is a right eigenvector. There are two families of eigenvalues (which we denote v_1 and v_2) and eigenvectors ($\mathbf{r}_1$ and $\mathbf{r}_2$). The eigenvalues and eigenvectors determine the character of the system.[13]

The system is called "hyperbolic" if, for each state $\mathbf{U}=(u,v)$, both eigenvalues $v_1(\mathbf{U})$ and $v_2(\mathbf{U})$ are real, and the Jacobian matrix $\mathbf{A}(\mathbf{U})$ is diagonalizable. If, in addition, the eigenvalues are distinct, $v_1(\mathbf{U})<v_2(\mathbf{U})$, the system is called "strictly hyperbolic." If there is a double eigenvalue and the Jacobian matrix is not diagonalizable, the system is "parabolic." Finally, if the eigenvalues are complex conjugates at some point $\mathbf{U}$, the system is "elliptic" at that point.

The eigenvalues are given by

$$v_{1,2}=\frac{1}{2}\left(f_{,u}+g_{,v}\mp\sqrt{(f_{,u}-g_{,v})^2+4f_{,v}g_{,u}}\right). \quad (20)$$

The eigenvalues are real whenever the discriminant is nonnegative, that is,

$$\delta := (f_{,u}-g_{,v})^2+4f_{,v}g_{,u}\geq 0, \quad (21)$$

and distinct if the inequality above is strict.

The eigenvectors $\mathbf{r}_p=[r_{pu},r_{pv}]^t$, $p=1,2$, of the system are given by the following expressions:

$$\frac{r_{1v}}{r_{1u}}=\frac{v_1-f_{,u}}{f_{,v}}=\frac{g_{,u}}{v_1-g_{,v}}, \quad (22)$$

$$\frac{r_{2u}}{r_{2v}}=\frac{f_{,v}}{v_2-f_{,u}}=\frac{v_2-g_{,v}}{g_{,u}}. \quad (23)$$

The eigenvectors should be normalized so that $|\mathbf{r}_p|\equiv 1$.

Three-Phase Relative Permeability Models

Introduction. We assume that pressure and temperature do not greatly influence fluid viscosities, and we take them as constants. Under this assumption, the character of the system is completely determined by the relative permeabilities.

Experimental evidence suggests that there is a threshold saturation for each phase, below which that phase is immobile. As a result, three-phase flow takes place only in a region inside the saturation triangle. The nature of these threshold saturations depends on the wettability of the fluid, and on the displacement process.[14] For the wetting phase, the term "connate" (or "irreducible") saturation would be appropriate both in drainage and imbibition. For the nonwetting phase, the term "critical" saturation would be applicable in drainage, and "trapped" (or "residual") saturation in imbibition. For the purpose of this paper we lump the terminology above in the term "immobile" saturation $S_{\alpha i}$, regardless of the process. If these endpoint saturations are taken as constants, one can define reduced saturations $\tilde{S}_\alpha$ as:

$$\tilde{S}_\alpha := \frac{S_\alpha - S_{\alpha i}}{1-\sum_{\beta=1}^{3} S_{\beta i}}, \quad \alpha=1,\ldots,3. \quad (24)$$

Eq. 24 defines a linear map from the three-phase flow subtriangle (the shaded region in **Fig. 2**) to the whole ternary diagram. It is important to note that the three-phase flow region is not necessarily an equilateral triangle, as the "immobile" saturation of each phase may vary with the saturations of the other two phases. This is a well-known behavior for the oil phase,[15] and several correlations for the "residual" oil saturation have been proposed.[16,17] In this case, the mapping of the three-phase flow region onto the unit ternary diagram would be more complicated than just the linear relation in Eqs. 24.

The relative permeability of a phase is zero if that phase is immobile, and it is positive otherwise. By expressing relative permeabilities as functions of reduced saturations, and using the linear transformation in Eq. 24, the original system in Eq. 13 can be written as:

$$\partial_t\tilde{\mathbf{u}}+\tilde{v}_T\partial_x\tilde{\mathbf{f}}(\tilde{\mathbf{u}})=0, \quad (25)$$

where $\tilde{\mathbf{f}}$ = the fractional flow vector expressed as a function of reduced saturations, and

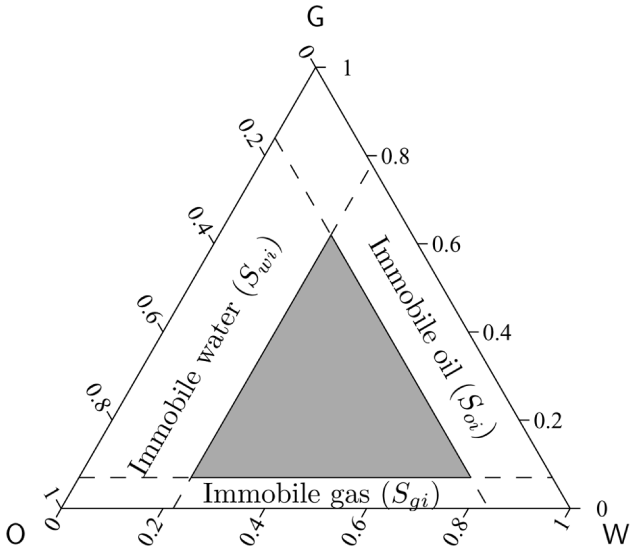

Fig 2—Schematic of constant immobile saturations for each phase. The three-phase flow region (shaded area) is, in this case, an equilateral triangle inside the ternary diagram.

$$\tilde{v}_T=\frac{v_T}{1-\sum_{\beta=1}^{3} S_{\beta i}} \quad (26)$$

is the reduced total velocity. To simplify notation, we shall drop the tildes from Eq. 25 but still refer to the system in terms of reduced saturations.

Loss of Strict Hyperbolicity in Conventional Models. The study of the character of the system was first addressed in the Russian literature. Charny[18] pointed out that for certain relative permeability functions, the system in Eq. 25 could be of mixed elliptic/hyperbolic type. He concluded, however, that the system is hyperbolic for realistic three-phase flows. This work did not permeate to the Western literature, where it was long believed that the system in Eq. 13 was hyperbolic for any relative permeability functions. Bell *et al.*[19] showed that the system is not necessarily hyperbolic. In particular, they observed that Stone I relative permeabilities gave rise to elliptic regions inside the saturation triangle. Elliptic regions are portions of the saturation triangle where the eigenvalues are complex, so the system is locally elliptic rather than hyperbolic. The analysis of Bell *et al.*[19] shows that the solution is unstable in these regions. One of the consequences is that for arbitrarily close initial and injected saturation states inside the elliptic region, the solution develops wildly oscillatory waves, which are not observed in experiments. Moreover, the wave pattern is unstable with respect to the initial states.

It was shown[17,20–24] that occurrence of elliptic regions is the rule rather than the exception for the most common relative permeability models. The analysis of Shearer[20] and Holden[23] starts by assuming the behavior of relative permeabilities at the edges of the saturation triangle. In particular, it is assumed that both the relative permeability of a phase, and its derivative along the normal to the edge of zero reduced saturation of that phase, are identically zero. In addition, certain "interaction conditions" are imposed. These conditions impose that the eigenvector parallel to the edge is the one associated with the fast characteristic speed, $\mathbf{r}_2$ **(Fig. 3).**

The assumed behavior at the edges has a profound impact on the character of the system. The first consequence is that each vertex of the saturation triangle is an umbilic point, at which eigenvalues are equal and the system is not strictly hyperbolic. The second consequence is that, in general, an elliptic region must exist inside the saturation triangle. This result can be proved using ideas of projective geometry.[20,25]

The only models that do not produce elliptic regions (under the assumed behavior at the edges) are those in which the relative

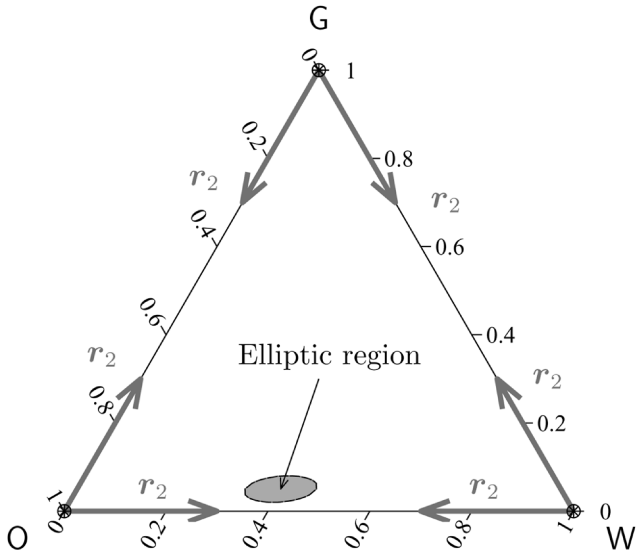

Fig. 3—Schematic representation of the direction of fast eigenvectors r_2 along the edges of the saturation triangle for the models analyzed by Shearer[20,21] and Holden.[23] For models of this type, vertices are umbilic points, and there must be an elliptic region inside the saturation triangle, usually very close to the oil-water edge.

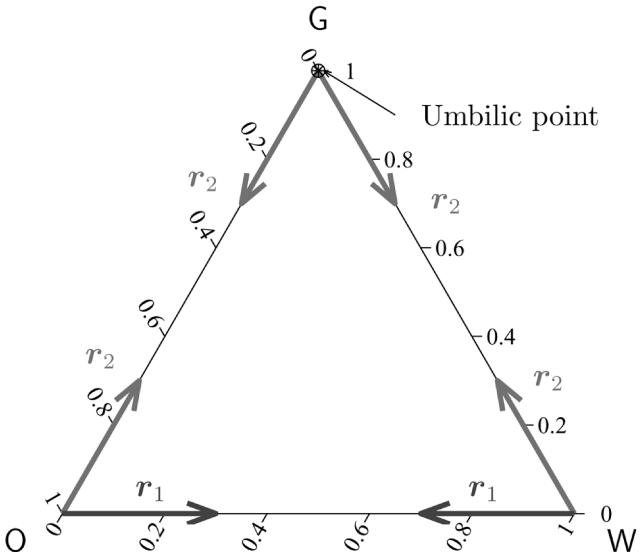

Fig. 4—Schematic representation of the direction of fast (r_2) and slow (r_1) eigenvectors along the edges of the saturation triangle for the type of models we propose. The system is strictly hyperbolic everywhere inside the saturation triangle, and the only umbilic point is located at the G vertex, where the fast paths corresponding to the OG and WG edges coalesce.

permeability of a phase depends solely on the saturation of that phase.[26,27] For these models, the elliptic region shrinks to an isolated umbilic point, which cannot be removed by further approximation of the relative permeabilities. Umbilic points act as "repellers" for classical waves,[28–30] and, as a result, solutions to the nonstrictly hyperbolic system require nonclassical waves (termed transitional waves[31]). Models of this type have been used also in the interpretation of three-phase displacement experiments.[32,33] However, the assumption that the relative permeabilities of all three phases depend solely on their respective saturations is not in agreement with pore-scale physics[34,35] and direct relative permeability measurements[36] (especially for the intermediate-wetting phase).

In a separate publication,[37] we provide very strong arguments supporting our view that elliptic regions are unphysical.[2,17,21,27,38–40] In our opinion, these singularities are mere artifacts of an incomplete mathematical model. Inappropriateness of the formulation may have several sources, the most obvious one being the relative permeability functions and, in particular, the assumed behavior at the edges of the saturation triangle. In fact, it is widely recognized that the slope of experimental relative permeabilities near the endpoints is often ill-defined.[17]

Description of the New Approach. The generic approach in the existing literature can be summarized as follows: a certain behavior of the relative permeabilities is "assumed," and loss of strict hyperbolicity inside the saturation triangle is "inferred." We adopt the opposite viewpoint: we assume that the system is strictly hyperbolic and investigate the conditions on relative permeabilities as functions of saturation such that strict hyperbolicity is preserved. Because the three-phase system must be consistent with the two-phase system when one of the phases is not mobile, the relative permeability of a phase must be identically equal to zero on the edge of zero reduced saturation of that phase. This obvious condition immediately implies that, on each edge of the saturation triangle, one of the eigenvectors is directed *along* the edge.

With this consideration in mind, the key observation is that, whenever gas is present as a continuous phase, the mobility of gas is usually much higher than that of the other two fluids (water and oil). To honor this physical behavior, we associate fast characteristic paths with displacements involving changes in gas saturation, even in the region of small gas saturation. The immediate consequence is that the eigenvector associated with the fast family of characteristics ($\mathbf{r}_2$) is transversal—and not parallel— to the oil-water (OW) edge of the ternary diagram **(Fig. 4).** This conceptual picture permits that the system be strictly hyperbolic everywhere inside the saturation triangle. The G vertex, corresponding to 100% reduced gas saturation, remains an umbilic point because fast paths corresponding to the OG and WG edges coalesce.

Therefore, the essential difference with respect to the models assumed in previous studies[20,23] is that along the OW edge, the eigenvector that is parallel to the edge is the one associated with the slow characteristic family ($\mathbf{r}_1$).

We have carried out a systematic study of the conditions for strict hyperbolicity. On each edge, we identify two types of conditions. Condition I enforces that eigenvectors of the appropriate family are parallel to the edge. Condition II guarantees strict hyperbolicity of the system along the edge. The latter condition is further specialized to both vertices of each edge, which provides additional insight into the behavior of the relative permeabilities. The analytical developments are expressed most effectively in terms of water and gas fractional flows (f and g, respectively) and their derivatives with respect to water and gas saturations (u and v, respectively). We then translate these requirements into conditions that must be satisfied by the relative permeabilities. We emphasize that relative permeabilities and, therefore, relative mobilities are assumed to be functions of saturations only; that is,

$$\lambda_w = \lambda_w(u,v),\ \lambda_g = \lambda_g(u,v),\ \lambda_o = \lambda_o(u,v). \quad \ldots\ldots\ldots\ldots\ldots\ldots (27)$$

Because of space restrictions, we present only the main results and their practical implications. The complete analysis is included in a separate publication.[37]

Analysis Along the OW Edge. This edge corresponds to the line of zero reduced gas saturation, $v = 0$. The conditions for strict hyperbolicity along this edge—and their particular form at the vertices—are summarized in **Table 1.** Condition I is immediately satisfied for any model, because the gas mobility is identically zero along this edge. Condition II, on the other hand, is the fundamental requirement for strict hyperbolicity of the system of equations of three-phase flow. Because the inequalities in Table 1 are strict, this condition dictates that the gas relative permeability must not have a zero derivative at its endpoint saturation. We make the following important remarks:

1. The requirement of a nonzero endpoint slope of the gas relative permeability is a necessary condition for strict hyperbo-

TABLE 1—SUMMARY OF CONDITIONS ALONG THE OW EDGE

Condition	Fractional Flows	Mobilities
I	$g_{,u}=0 \Leftrightarrow \lambda_{g,u}=0$	
II	$g_{,v}-f_{,u}>0 \Leftrightarrow \lambda_{g,v}>\lambda_{w,u}-\lambda_{T,u}\frac{\lambda_g}{\lambda_T}$	
II at O		$\lambda_{g,v}>\lambda_{w,u}$
II at W		$\lambda_{g,v}>-\lambda_{o,u}$

TABLE 2—SUMMARY OF CONDITIONS ALONG THE OG EDGE

Condition	Fractional Flows	Mobilities
I	$f_{,v}=0 \Leftrightarrow \lambda_{w,v}=0$	
II	$g_{,v}-f_{,u}>0 \Leftrightarrow \lambda_{g,v}>\lambda_{w,u}+\lambda_{T,v}\frac{\lambda_g}{\lambda_T}$	
II at O		$\lambda_{g,v}>\lambda_{w,u}$
II at W		$\lambda_{w,u}+\lambda_{o,v}=0$

licity, which is violated by the models of all previous studies on this subject.

2. This behavior of gas relative permeability is in good agreement with experimental observations of two-phase and three-phase flow, both in drainage and imbibition.[37]

3. A finite positive slope for the gas relative permeability, as well as a zero slope for the water relative permeability in a three-phase system, can also be justified from the point of view of pore-scale processes using a wettability argument.[37]

Analysis Along the OG Edge. This edge corresponds to the line of zero reduced water saturation, $u=0$. The conditions at the OG edge are summarized in **Table 2.** Condition I is immediately satisfied because water mobility is identically zero along this edge. Condition II involves a strict inequality at the O vertex:

$$\lambda_{g,v}>\lambda_{w,u}, \quad \ldots\ldots\ldots\ldots (28)$$

and an equality at the G vertex (umbilic point):

$$\lambda_{w,u}+\lambda_{o,v}=0. \quad \ldots\ldots\ldots\ldots (29)$$

Eq. 28 requires again that the gas relative permeability have a positive slope at its endpoint saturation.

Analysis Along the WG Edge. This edge corresponds to the line of zero reduced oil saturation, $v=1-u$. The relevant conditions are summarized in **Table 3.** As with the other two edges, Condition I is immediately satisfied because the oil relative permeability is identically zero along this edge. At the W vertex, Condition II is a strict inequality:

$$\lambda_{g,v}>-\lambda_{o,u}, \quad \ldots\ldots\ldots\ldots (30)$$

and at the G vertex (umbilic point) it reduces to the following equality:

$$\lambda_{w,u}+\lambda_{o,v}=0. \quad \ldots\ldots\ldots\ldots (31)$$

Table 3 summarizes the conditions at the WG edge.

A Simple Model. Our interest here reduces to presenting a simple model that satisfies the conditions above. A common practice in petroleum engineering[41,42] is to assume that relative permeabilities of the most-wetting and the least-wetting fluids (usually water and gas, respectively) depend only on their own saturation, whereas the relative permeability of the intermediate wetting fluid (usually oil) depends on all saturations. Although we do not defend this assumption in general, here we show that it is possible to obtain models which are strictly hyperbolic everywhere in the three-phase flow region. We take, for example:

$$\lambda_w=(1/\mu_w)u^2, \quad \ldots\ldots\ldots\ldots (32)$$

$$\lambda_g=(1/\mu_g)[\beta_g v+(1-\beta_g)v^2], \quad \beta_g>0 \quad \ldots\ldots\ldots\ldots (33)$$

$$\lambda_o=(1/\mu_o)(1-u-v)(1-u)(1-v). \quad \ldots\ldots\ldots\ldots (34)$$

The most important feature of the model is the positive derivative of the gas relative permeability function as it approaches zero. For the particular function used here, oil isoperms are slightly convex.[37]

It is straightforward to check that relative mobilities in Eqs. 32 through 34 satisfy Condition I on all three edges. Whether Condition II is satisfied will depend, in general, on the values of the fluid viscosities and the endpoint-slope of the gas relative permeability. Rather than performing a complete analysis,[37] we simply take reasonable values of the viscosities:

$$\mu_w=0.875, \quad \mu_g=0.03, \quad \mu_o=2, \quad \ldots\ldots\ldots\ldots (35)$$

and a small value of the endpoint slope: $\beta_g=0.1$.

In **Fig. 5,** we represent graphically the functions that define Condition II along each edge:

$$H_{ow}(u)=g_{,v}-f_{,u}>0 \quad \text{along OW}, \quad \ldots\ldots\ldots\ldots (36)$$

$$H_{og}(v)=g_{,v}-f_{,u}>0 \quad \text{along OG}, \quad \ldots\ldots\ldots\ldots (37)$$

$$H_{wg}(u)=-g_{,u}-f_{,v}>0 \quad \text{along WG}, \quad \ldots\ldots\ldots\ldots (38)$$

The inequalities above are satisfied (and the system is strictly hyperbolic) if all three curves are positive everywhere. The curves for the OG edge and the WG edge reach a zero value for $v=1$ and $u=0$, respectively, so the G vertex is an umbilic point.

TABLE 3—SUMMARY OF CONDITIONS ALONG THE WG EDGE

Condition	Fractional Flows	Mobilities
I	$f_{,v}+g_{,v}=f_{,u}+g_{,u} \Leftrightarrow \lambda_{o,v}=\lambda_{o,u}$	
II	$-g_{,u}-f_{,v}>0 \Leftrightarrow \frac{\lambda_o}{\lambda_T}(\lambda_{g,v}-\lambda_{g,u})+\frac{\lambda_g}{\lambda_T}(\lambda_{w,u}-\lambda_{w,v})>-\lambda_{o,u}$	
II at W		$\lambda_{g,v}>-\lambda_{o,u}$
II at G		$\lambda_{w,u}+\lambda_{o,v}=0$

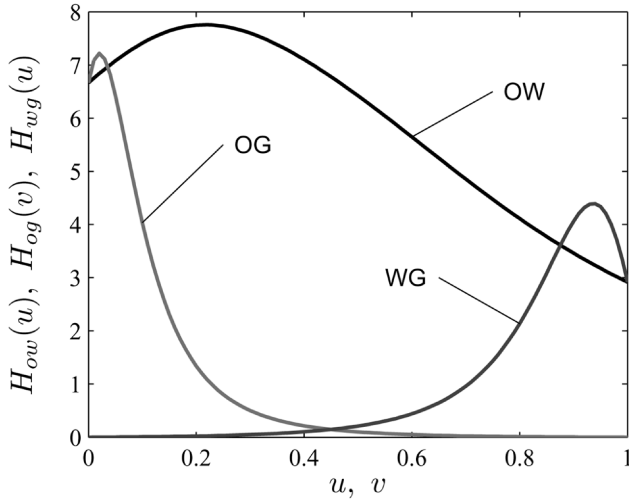

Fig. 5—Strict hyperbolicity on edges of the saturation triangle (Condition II) requires that all three functions $H_{ow}(u)$, $H_{og}(v)$, and $H_{wg}(u)$ are positive everywhere.

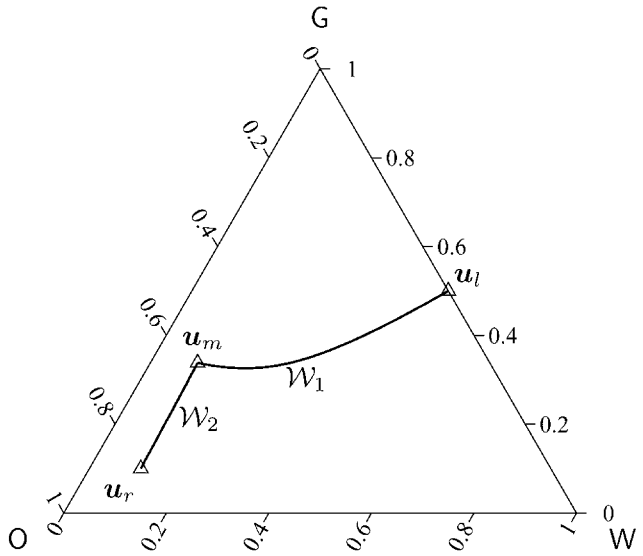

Fig. 6—Generic solution to the Riemann problem of three-phase flow with two waves connecting three constant states.

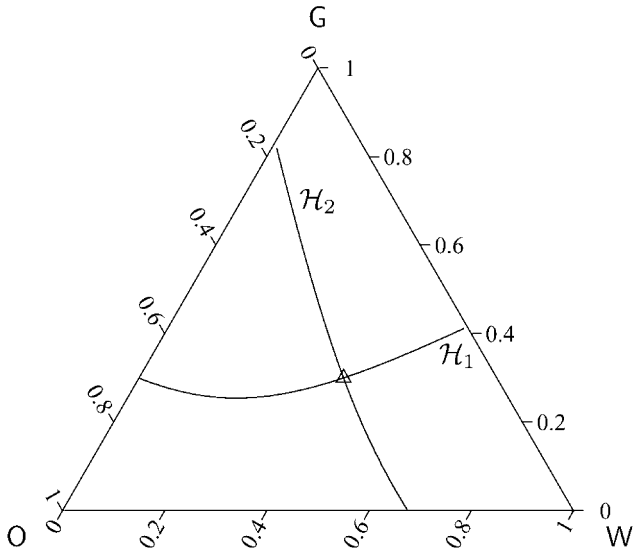

Fig. 7—Plot of the Hugoniot loci of both characteristic families passing through the reference state Δ.

Analytical Solution to the Riemann Problem

Introduction. Here we present the solution to the Riemann problem of three-phase flow given by Eqs. 13 and 14. As discussed in the previous section, the system is assumed to be strictly hyperbolic for all saturation paths of interest. The theory of strictly hyperbolic systems with characteristic fields that are either genuinely nonlinear or linearly degenerate was compiled by Lax.[43] It was then extended by Liu[44,45] to systems with nongenuinely nonlinear fields. This well-known theory is used here to find solutions to the three-phase flow Riemann problem. In an effort to make the developments accessible to the nonspecialized reader, we include in our discussion a review of the theory of strictly hyperbolic conservation laws.

For a strictly hyperbolic system, waves of different characteristic families are strictly separated.[43] Thus, the solution to the Riemann problem comprises three constant states $\mathbf{u}_l, \mathbf{u}_m, \mathbf{u}_r$ (left, middle, and right states, respectively). States $\mathbf{u}_l$ and $\mathbf{u}_m$ are joined by a wave of the first family (slow wave, or 1-wave), and states $\mathbf{u}_m$ and $\mathbf{u}_r$, are joined by a wave of the second family (fast wave, or 2-wave). Therefore, the solution to the Riemann problem for three-phase flow reduces to finding the intermediate constant state $\mathbf{u}_m$ as the intersection of an admissible 1-wave (W_1) and an admissible 2-wave (W_2) on the saturation triangle **(Fig. 6):**

$$\mathbf{u}_l \xrightarrow{w_1} \mathbf{u}_m \xrightarrow{w_2} \mathbf{u}_r. \quad \ldots\ldots\ldots\ldots\ldots\ldots\ldots\ldots\ldots\ldots\ldots\ldots\ldots\ldots (39)$$

Wave Structure. We now describe the structure of the waves in the Riemann solution. From the theory of strictly hyperbolic conservation laws,[43,46] a wave of the p-family consists of p-rarefactions, p-shocks, and/or p-contact discontinuities. This is discussed next.

Hugoniot Loci and Shocks. Any propagating discontinuity connecting two states $\mathbf{u}_- = \mathbf{U}(\zeta_-)$ and $\mathbf{u}_+ = \mathbf{U}(\zeta_+)$ must satisfy an integral conservation equation for each variable, known as the Rankine-Hugoniot jump condition[7,46]:

$$\mathbf{f}(\mathbf{u}_+) - \mathbf{f}(\mathbf{u}_-) = \sigma(\mathbf{u}_+;\mathbf{u}_-)(\mathbf{u}_+ - \mathbf{u}_-), \quad \ldots\ldots\ldots\ldots\ldots\ldots\ldots\ldots\ldots\ldots (40)$$

where $\sigma(\mathbf{u}_+;\mathbf{u}_-)$ is the speed of propagation of the discontinuity. For a fixed state $\mathbf{u}_-$, one can determine the set of states $\mathbf{u}_+$ that can be connected to $\mathbf{u}_-$ so that Eq. 40 is satisfied. There are two families of solutions, one for each characteristic family, which form two curves passing through the reference state $\mathbf{u}_-$:$H_1(\mathbf{u}_-)$ and $H_2(\mathbf{u}_-)$ **(Fig. 7).** The set of points on each of these curves is called the Hugoniot locus. It is easy to show[7] that the Hugoniot curves are tangent to the corresponding eigenvectors at the reference point $\mathbf{u}_-$. Moreover, in our case, Hugoniot loci are also transversal to each other.[46]

Not every discontinuity satisfying the Rankine-Hugoniot condition is a valid shock. For a genuine shock of the p-family (a p-shock) to be physically admissible, it must satisfy the Lax entropy condition[7,43]:

$$v_p(\mathbf{u}_-) > \sigma_p(\mathbf{u}_+;\mathbf{u}_-) > v_p(\mathbf{u}_+), \quad \ldots\ldots\ldots\ldots\ldots\ldots\ldots\ldots\ldots\ldots (41)$$

where $\mathbf{u}_-$ and $\mathbf{u}_+$ are the values at the left and at the right of the discontinuity, respectively. Condition 41 implies that characteristics of the p-family go *into* the shock. A shock curve of the p-family passing through point $\mathbf{u}_-$, denoted as $S_p(\mathbf{u}_-)$, corresponds to a subset of the Hugoniot locus $H_p(\mathbf{u}_-)$, for which entropy condition Eq. 41 is satisfied.

Integral Curves and Rarefactions. A curve whose tangent at any point $\mathbf{u}$ lies in the direction of the right eigenvector $\mathbf{r}_p(\mathbf{u})$ is called an integral curve for the p-family. There are two integral curves passing through each reference point $\hat{\mathbf{u}}$:$I_1(\hat{\mathbf{u}})$, corresponding to the first eigenvector $\mathbf{r}_1$, and $I_2(\hat{\mathbf{u}})$, corresponding to the second eigenvector $\mathbf{r}_2$. The two families of integral curves for the relative permeability model discussed in the previous section (Eqs. 32 and 33) are shown in **Fig. 8.**

A necessary condition for two states $\mathbf{u}_l$ (left) and $\mathbf{u}_r$ (right) to be connected by a rarefaction wave is that these two states lie on the same integral curve.[7,43] Therefore, a rarefaction curve of the p-family (hereafter noted R_p), is a subset of integral curve I_p, much in the same way as a shock curve is a subset of the corresponding Hugoniot locus. A p-rarefaction wave is a self-similar solution $\mathbf{U}_p(\zeta)$ satisfying Eq. 17 where the parameter ζ is not arbitrary, but an eigenvalue of the problem[7]

$$\zeta = v_p[\mathbf{U}_p(\zeta)]. \quad \ldots\ldots\ldots\ldots\ldots\ldots\ldots\ldots\ldots\ldots\ldots\ldots\ldots\ldots (42)$$

A rarefaction curve $\mathbf{U}_p(\zeta)$ will provide a single-valued solution if the similarity variable parameter ζ (that is, the eigenvalue v_p) increases monotonically along the curve from the left state $\mathbf{u}_l$ to the right state $\mathbf{u}_r$.

Inflection Loci and Rarefaction-Shocks. The notion of genuine nonlinearity is crucial to the wave structure arising in multiphase flow. The p-field is said to be genuinely nonlinear if the p-eigenvalue v_p varies monotonically along integral curves of the p-family. This is expressed mathematically as

$$\nabla v_p(\mathbf{U}) \cdot \mathbf{r}_p(\mathbf{U}) \neq 0 \quad \text{for all } \mathbf{U}, \quad \ldots\ldots\ldots\ldots\ldots\ldots\ldots\ldots (43)$$

where $\nabla v_p(\mathbf{U}) := [\partial v_p/\partial u, \partial v_p/\partial v]^t$ is the gradient of $v_p(\mathbf{U})$. This condition is equivalent to that of convexity, $f''(u) \neq 0 \forall \mu$, for scalar conservation laws. The p-field is said to be linearly degenerate if v_p is constant along integral curves of the p-family; that is,

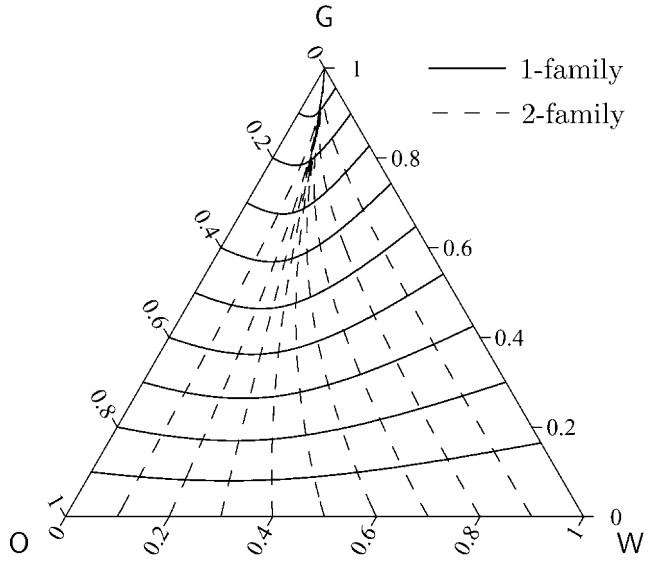

Fig. 8—Plot of the integral curves (usually termed slow paths and fast paths) for a relative permeability model that produces a strictly hyperbolic system.

$$\nabla v_p(\mathbf{U}) \cdot \mathbf{r}_p(\mathbf{U}) \equiv 0 \quad \text{for all } \mathbf{U}. \ldots\ldots\ldots\ldots\ldots\ldots\ldots\ldots (44)$$

Of course, the value of $v_p(\mathbf{U})$ may vary from one integral curve to the next. The characteristic fields of the system describing three-phase flow are neither genuinely nonlinear nor linearly degenerate: eigenvalues attain local maxima along integral curves. The inflection locus V_p for the p-characteristic field is defined as the set of points $\mathbf{U}$ so that

$$\nabla v_p(\mathbf{U}) \cdot \mathbf{r}_p(\mathbf{U}) = 0; \ldots\ldots\ldots\ldots\ldots\ldots\ldots\ldots\ldots\ldots (45)$$

that is, the locations at which v_p attain either a maximum or a minimum value when moving along integral curves of the p-family. In **Fig. 9** we show contour plots of eigenvalues and the inflection loci for both characteristic families. We note that in realistic models of multiphase flow, the inflection locus corresponds to maxima of eigenvalues. This is consistent with the common behavior of the flux function for the two-phase flow case, where the fractional-flow function is S-shaped, and the inflection point corresponds to the maximum value of the derivative **(Fig. 10).**

For a strictly hyperbolic system whose characteristic fields are genuinely nonlinear, any wave connecting two states $\mathbf{u}_l$ and $\mathbf{u}_r$ can only be a rarefaction or a genuine shock, and any discontinuity must satisfy the Lax entropy condition in Eq. 41. When the genuine nonlinearity condition is not satisfied, each wave might consist of a combination of rarefactions and discontinuities.[44,45] For the strictly hyperbolic models of multiphase flow we propose, the inflection locus for each field is a single connected curve, which is transversal to integral curves of the same family. In this case, the composite wave has at most one rarefaction and one discontinuity. Moreover, because inflection loci correspond to local maxima of eigenvalues along integral curves, the rarefaction is always slower than the shock.[47] Therefore, a wave consisting of a shock followed by a rarefaction is not possible.

More precisely, a rarefaction-shock of the p-family connecting the left and right states $\mathbf{u}_l$ and $\mathbf{u}_r$, respectively, is a curve on the phase plane consisting of a p-rarefaction curve emanating from $\mathbf{u}_l$, connected to a p-shock curve at some intermediate point $\mathbf{u}_*$, which ends at the right state. This rarefaction-shock curve is denoted as $R_pS_p(\mathbf{u}_r;\mathbf{u}_l)$ and, unlike rarefaction curves or shock curves alone, is defined through both endpoints. The intermediate state $\mathbf{u}_*$ is the postshock state, at which the following property holds:

$$v_p(\mathbf{u}_*) = \sigma_p(\mathbf{u}_r;\mathbf{u}_*). \ldots\ldots\ldots\ldots\ldots\ldots\ldots\ldots\ldots\ldots (46)$$

A necessary condition for an $R_pS_p(\mathbf{u}_r;\mathbf{u}_l)$ wave is that the left and right states lie on opposite sides with respect to the inflection locus

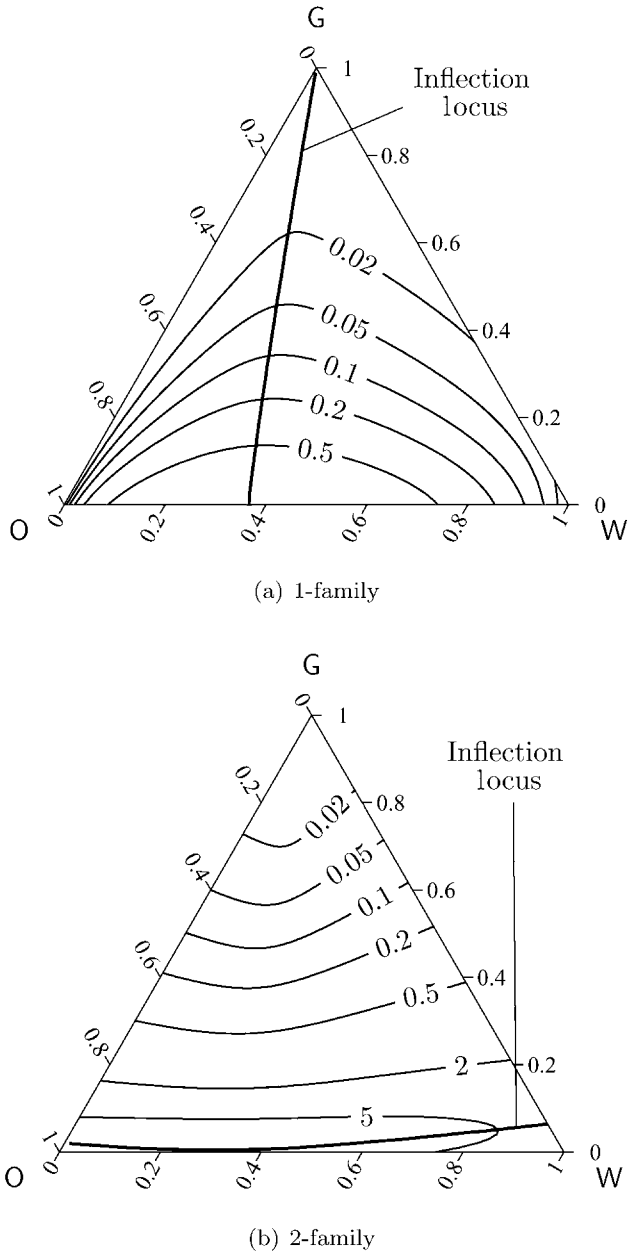

Fig. 9—Eigenvalues and inflection loci for both families of characteristics. Inflection loci correspond to local maxima of eigenvalues when moving along integral curves.

V_p. This rules out the possibility of such two states being connected by a rarefaction wave, because the characteristic speed would not be monotonically increasing, and, as a result, the solution would not be single-valued. This composite wave also satisfies Liu's extended entropy condition,[44] which reduces to the extended Lax entropy condition[43] (originally developed for systems with genuinely nonlinear and linearly degenerate fields) when the inflection locus is a single hypersurface.[47] Therefore, all discontinuities must satisfy

$$v_p(\mathbf{u}_-) \geq \sigma_p(\mathbf{u}_+;\mathbf{u}_-) > v_p(\mathbf{u}_+). \ldots\ldots\ldots\ldots\ldots\ldots\ldots\ldots (47)$$

Fig. 11 shows two rarefaction-shock curves for the first characteristic family, corresponding to the same left state but two different right states. Note that the postshock state $\mathbf{u}_*$, at which the R_1 and S_1 curves are connected, is different for each case. This connection is always very smooth. In fact, it can be shown[43] that both curves are connected with second-order tangency (same slope and curvature).

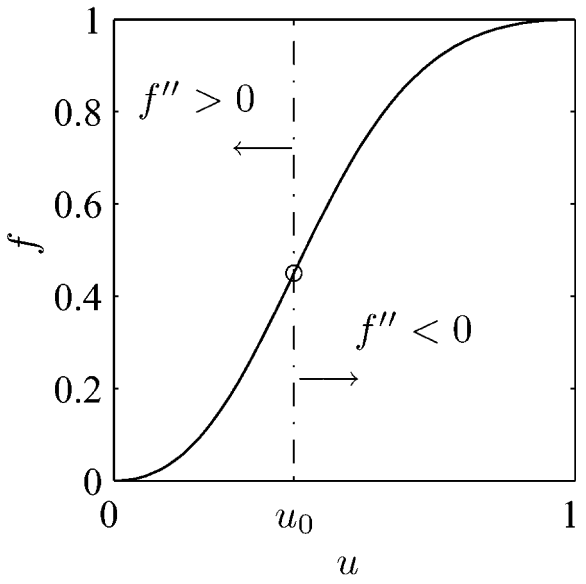

Fig. 10—Typical plot of the flux function *f* (fractional flow) for two-phase flow. The function is S-shaped, and the slope attains a maximum value at the inflection point u_0.

Complete Set of Solutions. Based on the analysis above, a wave of the *p*-family connecting two constant states may only be one of the following: a *p*-rarefaction (R_p), a *p*-shock (S_p), or a *p*-rarefaction-shock (R_pS_p). Because the full solution to the Riemann problem is a sequence of two waves, W_1 and W_2, there are only nine possible combinations of solutions. A schematic tree with all possible solution types is shown in **Fig. 12.**

***Example:* $R_1S_1R_2S_2$ Solution.** We describe in some detail the case with the most complicated wave structure that may arise in the Riemann problem of three-phase flow. In this case, both waves are composite rarefaction-shocks: $W_1 \equiv R_1S_1$ and $W_2 \equiv R_2S_2$.

The variables that need to be determined to fully characterize the solution are the intermediate constant state $\mathbf{u}_m$, the shock speeds σ_1 and σ_2, and the postshock states $\mathbf{u}_1^*$ and $\mathbf{u}_2^*$ of each wave. The constant state $\mathbf{u}_m$ corresponds to the intersection of the two wave curves, while the postshock states are the points at which the rarefaction curve and the shock curve of the same family are joined. Schematically, this can be represented as follows:

$$\mathbf{u}_l \xrightarrow{R_1} \mathbf{u}_1^* \xrightarrow{S_1} \mathbf{u}_m \xrightarrow{R_2} \mathbf{u}_2^* \xrightarrow{S_2} \mathbf{u}_r. \quad \ldots\ldots\ldots\ldots\ldots\ldots (48)$$

The solution is admissible if each of the two waves is admissible individually; that is,

$$R_1S_1: \begin{cases} v_1 \text{ increases monotonically along } \mathbf{u}_l \xrightarrow{R_1} \mathbf{u}_1^*, \\ v_1(\mathbf{u}_1^*) = \sigma_1 > v_1(\mathbf{u}_m), \end{cases} \quad \ldots (49)$$

$$R_2S_2: \begin{cases} v_2 \text{ increases monotonically along } \mathbf{u}_m \xrightarrow{R_2} \mathbf{u}_2^*, \\ v_2(\mathbf{u}_2^*) = \sigma_2 > v_2(\mathbf{u}_r). \end{cases} \quad \ldots\ldots\ldots\ldots\ldots\ldots\ldots (50)$$

The major difficulty in computing the solution is that both endpoints of the R_2 curve are unknown, so that the initial condition for the integral curve is not known a priori. We have developed efficient algorithms for the solution of this highly nonlinear problem. They are based on a predictor-corrector strategy combined with Newton's method, and they yield quadratic convergence in all cases.[48]

In **Fig. 13,** we represent the solution as a saturation path in the ternary diagram. It is immediate to check that the solution is admissible. Each composite wave crosses the inflection locus of the corresponding family. We note that the 2-shock has very small amplitude because the right state almost coincides with the inflection locus of the 2-family.

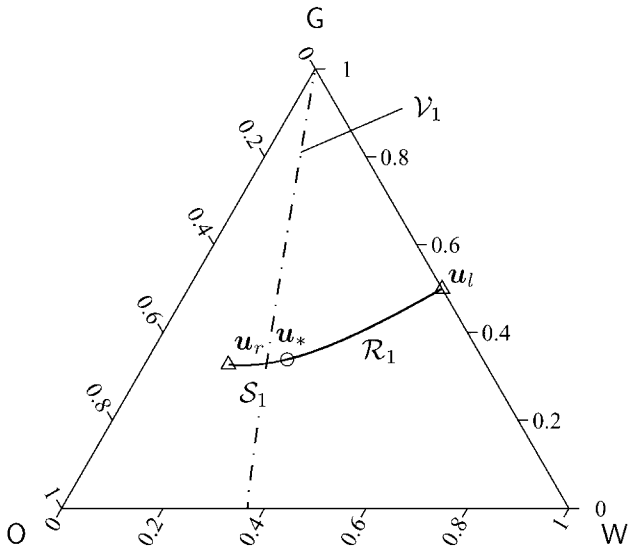

(a) Right state with $u_r \approx 0.17$

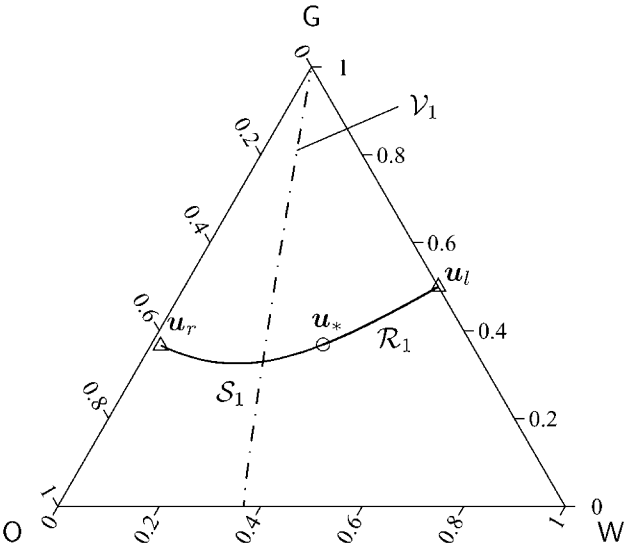

(b) Right state with $u_r \approx 0.02$

Fig. 11—Rarefaction-shock curves for the 1-family with the same left state and two different right states. Note that the postshock state $\mathbf{u}_*$ is different for each case.

Profiles of wave speeds v_1. and v_2, and phase saturations S_w, S_g, and S_o are plotted in **Fig. 14.** These quantities are plotted against the similarity variable ζ defined in Eq. 16. We decided to split each plot into two and use a different scale on the ζ-axis, because of the very different speeds of the 1- and 2-wave. Otherwise, the structure of the 1-rarefaction-shock would not be visible on the plots. Points $a<b<c<d$ on the ζ-axis correspond to the wave speeds $v_1(\mathbf{u}_l)<\sigma_1<v_2(\mathbf{u}_m)<\sigma_2$.

Remaining Types of Solution. For completeness, we present in **Fig. 15** the saturation paths in the ternary diagram for all nine solution types. These are:

1. S_1S_2: Both waves are genuine shocks, and, therefore, the solution comprises three constant states separated by two discontinuities.
2. S_1R_2: The solution consists of a 1-shock and a 2-rarefaction.
3. $S_1R_2S_2$: The solution comprises a genuine 1-shock through the left state and a composite 2-rarefaction-shock through the right state.

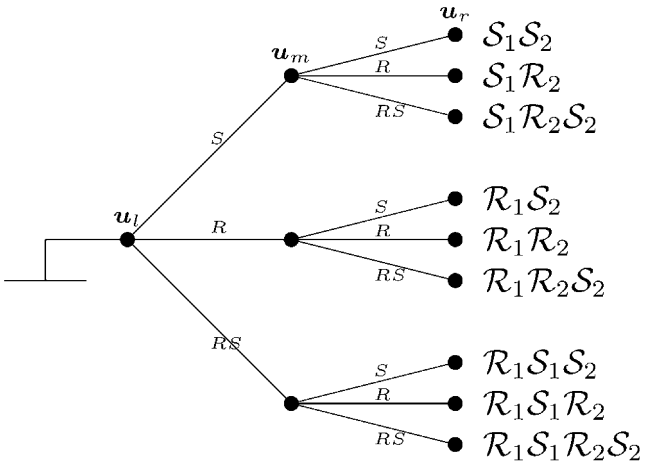

Fig. 12—Schematic tree with all nine possible combinations of solutions to the Riemann problem of three-phase flow.

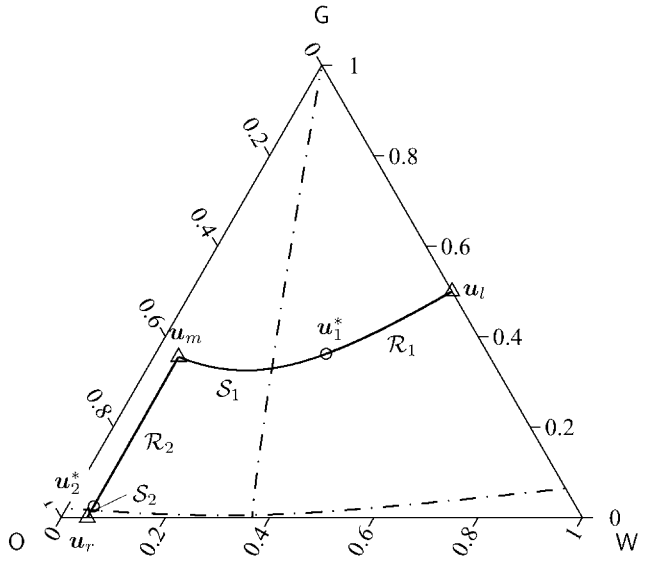

Fig. 13—$R_1S_1R_2S_2$ solution path in the ternary diagram. Both waves are rarefaction-shocks, which intersect at the intermediate constant state u_m. The postshock states u_1^* and u_2^* correspond to the points at which the rarefaction curve and the shock curve of the same family are joined.

4. R_1S_2: The left state and the right state are joined by a 1-rarefaction followed by a 2-shock.

5. R_1R_2: Both waves are rarefactions, so the solution is continuous everywhere.

6. $R_1R_2S_2$: A 1-rarefaction from the left state is followed by a composite 2-rarefaction-shock to the right state.

7. $R_1S_1S_2$: The slow wave emanating from the left state is a composite rarefaction-shock, which is followed by a genuine 2-shock to the right state.

8. $R_1S_1R_2$: The left state is joined to the intermediate constant state by a composite rarefaction-shock, and the right state is reached along a 2-rarefaction.

9. $R_1S_1R_2S_2$: Both waves are rarefaction-shocks.

All cases discussed above give a complete set of solutions to the Riemann problem of three-phase flow, under the following assumptions: (1) the system is strictly hyperbolic; and (2) inflection loci are single connected curves, transversal to the integral curves, and correspond to maxima of the eigenvalues.

The widely used conceptual model of three-phase flow as consisting of two successive two-phase flow displacements[10,49,50] can now be understood in the context of the complete solution. This model is an approximation to the actual solution, which assumes that each wave (W_1 and W_2) is parallel to one of the edges of the ternary diagram. This approximation is accurate only under very restrictive initial and injected conditions.[48]

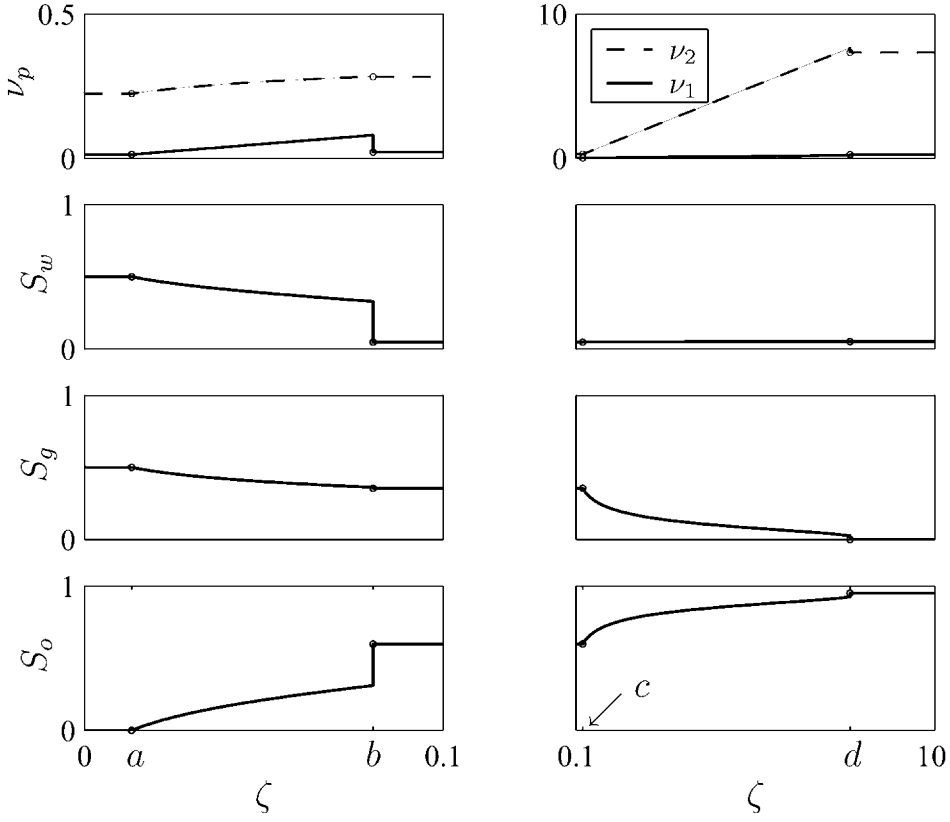

Fig. 14—Profiles of wave speeds v_1 and v_2, and phase saturations S_w, S_g, and S_o, for the $R_1S_1R_2S_2$ solution. The solution is plotted against the similarity variable ζ. Points $a<b<c<d$ on the ζ-axis correspond to the wave speeds $v_1(u_l)<\sigma_1<v_2(u_m)<\sigma_2$.

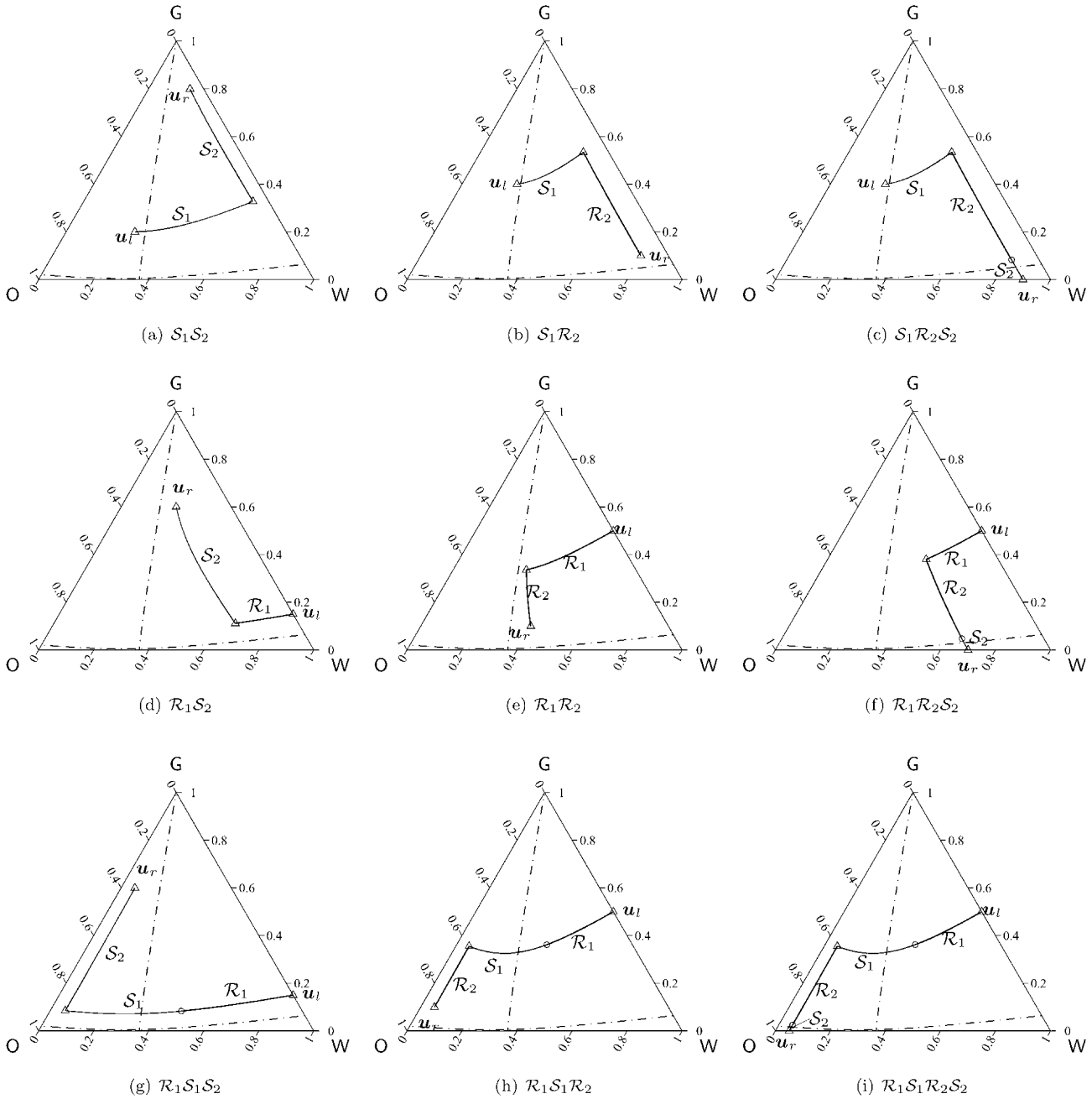

Fig. 15—Examples of saturation paths for all nine solution types. These nine cases constitute the complete set of solutions to the Riemann problem of three-phase flow.

Conclusions

Following the unambiguous hints from physics, we have first assumed the hyperbolicity of the system of equations describing three-phase immiscible flow, and then investigated the conditions on relative permeabilities that follow from this assumption. The mathematical derivations presented here lead to meaningful conditions that agree with experimental observations and pore-scale physics.[37] Our paper has two key results:

1. The derivation of general conditions on relative permeabilities necessary to preserve strict hyperbolicity.
2. The presentation of the complete solution to the Riemann problem of three-phase, incompressible, and immiscible flow, under the assumptions that the system is strictly hyperbolic and that the inflection loci are single connected curves corresponding to maxima of eigenvalues.

It turns out that a physically reasonable requirement of a finite positive slope of the gas relative permeability function is the most serious condition that must be imposed, so that all three relative permeabilities yield a strictly hyperbolic system everywhere in the three-phase flow region. For a commonly used model of three-phase relative permeabilities, reasonable values of fluid viscosities are sufficient to preserve strict hyperbolicity. The analysis presented here has recently been extended to the case of cocurrent three-phase flow with gravity.[51]

We have shown that, under certain physical conditions, the complete solution to the Riemann problem of three-phase immiscible, incompressible flow with negligible capillarity and gravity, involves a sequence of two waves, and that each wave may only be a rarefaction, a shock, or a rarefaction-shock. Thus, there can be only nine possible combinations of the admissible waves. All these combinations are discussed in our paper. Moreover, the widely used model of three-phase displacement as two successive two-phase displacements is identified as an approximation to the full solution. Such approximation is sufficiently accurate only under very restrictive conditions.[48]

The results of this paper will be useful for the following:

- Planning and interpretation of three-phase displacement experiments.
- Obtaining significantly more information from the existing displacement experiments.
- Designing the first complete analytical forward simulator to interpret three-phase displacement experiments.
- Formulating better relative permeability models.
- Formulating efficient streamline simulators of three-phase flow.[52,53]

Nomenclature

$\mathbf{A}$ = Jacobian matrix of the system, dimensionless
f = water fractional flow, dimensionless
f_α = fractional flow of the α phase, dimensionless
$\mathbf{f}$ = fractional flow vector $[f,g]=[f_w,f_g]$, dimensionless
F_α = mass flux of the α phase, m/L^{2}t
g = gas fractional flow, dimensionless
g = gravitational acceleration, L/t^2
H_p = Hugoniot locus of the p-characteristic family
I_p = integral curve of the p-characteristic family
$\mathbf{I}$ = 2×2 identity matrix, dimensionless
k = absolute permeability, L^2
$k_{r\alpha}$ = relative permeability of the α phase, dimensionless
m_α = mass of the α phase p.u. bulk volume, m/L^3
p = global pressure, m/Lt^2
p_α = pressure of the α phase, m/Lt^2
$\mathbf{r}_p$ = eigenvector of the p family, dimensionless
R_p = rarefaction curve of the p-characteristic family
S_p = shock curve of the p-characteristic family
S_α = saturation of the α phase, dimensionless
$S_{\alpha i}$ = immobile saturation of the α phase, dimensionless
$\tilde{S}_\alpha$ = reduced saturation of the α phase, dimensionless
t = time, t
T = saturation triangle
u = water saturation S_w, *dimensionless*
$\mathbf{u}$ = vector of saturations $[u,v]=[S_w,S_g]$, dimensionless
$\tilde{\mathbf{u}}$ = vector of reduced saturations, dimensionless
$\mathbf{U}$ = self-similar solution $[u,v]$, dimensionless
v = gas saturation S_g, dimensionless
v_T = total velocity, L/t
$\tilde{v}_T$ = reduced total velocity, L/t
v_α = velocity of the α phase, L/t
V_p = inflection locus of the p-characteristic family
W_p = wave of the p-characteristic family
x = space coordinate, L
z = vertical coordinate, L
δ = discriminant of the eigenvalue problem, dimensionless
ζ = self-similarity variable, dimensionless
λ_T = total mobility, Lt/m
λ_α = relative mobility of the α phase, Lt/m
μ_α = dynamic viscosity of the α phase, m/Lt
ν_p = eigenvalue of the p family, dimensionless
ρ_α = density of the α phase, m/L^3
σ_p = speed of a shock of the p-characteristic family, dimensionless
ϕ = porosity, dimensionless

Subscripts

g = gas phase
l = left state
m = intermediate constant state
o = oil phase
r = right state
$,u$ = partial derivative w.r.t. u
w = water phase
1 = 1-characteristic family
2 = 2-characteristic family
+ = state to the right of a discontinuity
– = state to the left of a discontinuity
* = post-shock state

Acknowledgments

This work was supported in part by the U.S. Department of Energy under Contract No. DE-AC03-76SF00098. Funding provided by the Jane Lewis Fellowship and the Repsol-YPF Fellowship, awarded to the first author, is gratefully acknowledged.

References

1. DiCarlo, D.A., Sahni, A., and Blunt, M.J.: "The effect of wettability on three-phase relative permeability," *Transp. Porous Media* (2000) **39,** 347.
2. Chavent, G. and Jaffré, J.: *Mathematical Models and Finite Elements for Reservoir Simulation,* Elsevier, Amsterdam (1986).
3. Truesdell, C.: *An Idiot's Fugitive Essays on Science—Methods, Criticism, Training, Circumstances,* Springer-Verlag, New York City (1984).
4. Aziz, K. and Settari, A.: *Petroleum Reservoir Simulation,* Elsevier, London (1979).
5. Muskat, M.: *Physical Principles of Oil Production,* McGraw-Hill, New York City (1949).
6. Godunov, S.K.: "A difference scheme for numerical computation of discontinuous solutions of equations of fluid dynamics," (in Russian), *Mat. Sb.* (1959) **47,** No. 89, 271.
7. LeVeque, R.J.: *Numerical Methods for Conservation Laws,* second edition, Birkhäuser Verlag, Berlin (1992).
8. Holden, H. and Risebro, N.H.: *Front Tracking for Hyperbolic Conservation Laws,* Springer, New York City (2002).
9. Welge, H.J.: "A Simplified Method for Computing Oil Recovery by Gas or Water Drive," *Trans.,* AIME (1952) 91, **195.**
10. Pope, G.A.: "The Application of Fractional Flow Theory to Enhanced Oil Recovery," *SPEJ* (June 1980) 191, *Trans.,* AIME, **269.**
11. Helfferich, F.G.: "Theory of Multicomponent, Multiphase Displacement in Porous Media," *SPEJ* (February 1981) 51, *Trans.,* AIME, **271.**
12. Barenblatt, G.I.: *Scaling, Self-Similarity, and Intermediate Asymptotics,* Cambridge U. Press (1996).
13. Zauderer, E.: *Partial Differential Equations of Applied Mathematics,* John Wiley & Sons, New York City (1983).
14. Geffens, T.M., Owens, W.W., Parrish, D.R., and Morse, R.A.: "Experimental Investigation of Factors Affecting Laboratory Relative Permeability Measurements," *Trans.,* AIME (1951) 99, **192.**
15. Land, C.S.: "Calculation Of Imbibition Relative Permeability for Two- and Three-Phase Flow From Rock Properties," *SPEJ* (June 1968) 149; *Trans.,* AIME, **243.**
16. Fayers, F.J. and Matthews, J.D.: "Evaluation of Normalized Stone's Methods for Estimating Three-Phase Relative Permeabilities," *SPEJ* (April 1984) 224; *Trans.,* AIME, **277.**
17. Fayers, F.J.: "Extension of Stone's Method I and Conditions for Real Characteristics in Three-Phase Flow," *SPERE* (November 1989) 437; *Trans.,* AIME, **287.**
18. Charny, I.A.: *Subterranean Hydro-Gas Dynamics,* (in Russian), Gostoptekhizdat, Moscow (1963).
19. Bell, J.B., Trangenstein, J.A., and Shubin, G.R.: "Conservation laws of mixed type describing three-phase flow in porous media," *SIAM J. Appl. Math.* (1986) **46,** No. 6, 1000.
20. Shearer, M.: "Loss of strict hyperbolicity of the Buckley-Leverett equations for three phase flow in a porous medium," *Numerical Simulation in Oil Recovery,* M.F. Wheeler (ed.), Springer-Verlag, New York City (1988) 263–283.
21. Shearer, M. and Trangenstein, J.A.: "Loss of real characteristics for models of three-phase flow in a porous medium," *Transp. Porous Media* (1989) **4,** 499.
22. Holden, L.: "On the strict hyperbolicity of the Buckley-Leverett equations for three-phase flow," *Nonlinear Evolution Equations That Change Type*, B.L. Keyfitz and M. Shearer (eds.), Springer-Verlag, New York City (1990) 79–84.

23. Holden, L.: "On the strict hyperbolicity of the Buckley-Leverett equations for three-phase flow in a porous medium," *SIAM J. Appl. Math.* (1990) **50,** No. 3, 667.
24. Hicks, P.J. Jr., and Grader, A.S.: "Simulation of three-phase displacement experiments," *Transp. Porous Media* (1996) **24,** 221.
25. Schaeffer, D.G. and Shearer, M.: "The classification of 2×2 systems of nonstrictly hyperbolic conservation laws, with application to oil recovery," *Comm. Pure Appl. Math.* (1987) **40,** No. 1, 141, Appendix with D. Marchesin and P.J. Paes-Leme.
26. Marchesin, D. and Medeiros, H.B.: "A note on the stability of eigenvalue degeneracy in nonlinear conservation laws of multiphase flow," *Current Progress in Hyperbolic Systems: Riemann Problems and Computations*, W.B. Lindquist (ed.), American Mathematical Soc., Providence, Rhode Island (1989) 215–224.
27. Trangenstein, J.A.: "Three-phase flow with gravity," *Current Progress in Hyperbolic Systems: Riemann Problems and Computations,* W.B. Lindquist (ed.), American Mathematical Soc., Providence, Rhode Island (1989) 147–159.
28. Guzmán, R.E. and Fayers, F.J.: "Mathematical Properties of Three-Phase Flow Equations," *SPEJ* (September 1997) 291.
29. Guzmán, R.E. and Fayers, F.J.: "Solutions to the Three-Phase Buckley-Leverett Problem," *SPEJ* (September 1997) 301.
30. Marchesin, D. and Plohr, B.J.: "Wave Structure in WAG Recovery," *SPEJ* (June 2001) 209.
31. Isaacson, E., Marchesin, D., and Plohr, B.: "Transitional shock waves," *Current Progress in Hyperbolic Systems: Riemann Problems and Computations,* W.B. Lindquist (ed.), American Mathematical Soc., Providence, Rhode Island (1989) 125–145.
32. Grader, A.S. and O'Meara, D.J. Jr.: "Dynamic Displacement Measurements of Three-Phase Relative Permeabilities Using Three Immiscible Fluids," paper SPE 18293 presented at the 1988 SPE Annual Technical Conference and Exhibition, Houston, 2–5 October.
33. Sahni, A., Guzmán, R., and Blunt, M.: "Theoretical Analysis of Three-Phase Flow Experiments in Porous Media," paper SPE 36664 presented at the 1996 SPE Annual Technical Conference and Exhibition, Denver, 6–9 October.
34. Al-Futaisi, A. and Patzek, T.W.: "Impact of oil-water drainage and imbibition on subsequent gas injection: A three-phase pore network model," *Phys. Rev. E* (2003) (in review).
35. van Dijke, M.I.J., Sorbie, K.S., and McDougall, S.R.: "Saturation-dependencies of three-phase relative permeabilities in mixed-wet and fractionally wet systems," *Adv. Water Resour.* (2001) **24,** 365.
36. Oak, M.J.: "Three-Phase Relative Permeability of Water-Wet Berea," paper SPE 20183 presented at the 1990 SPE/DOE Seventh Symposium on Enhanced Oil Recovery, Tulsa, 22–25 April.
37. Juanes, R. and Patzek, T.W.: "Relative permeabilities for strictly hyperbolic models of three-phase flow in porous media," *Transp. Porous Media* (2004) **57,** No. 2, 125.
38. Chavent, G., Jaffré, J., and Jan-Jégou, S.: "Estimation of relative permeabilities in three-phase flow in porous media," *Inverse Problems* (1999) **15,** 33.
39. Miller, C.T., Christakos, G., Imhoff, P.T., McBride, J.F., Pedit, J.A., and Trangenstein, J.A.: "Multiphase flow and transport modeling in heterogeneous porous media: challenges and approaches," *Adv. Water Resour.* (1998) **21,** No. 2, 77.
40. Azevedo, A.V., Marchesin, D., Plohr, D., and Zumbrun, K.: "Capillary instability in models for three-phase flow," *Z. angew. Math. Phys.* (2002) **53,** 713.
41. Stone, H.L.: "Probability Model for Estimating Three-Phase Relative Permeability," *JPT* (February 1970) 214; *Trans.,* AIME, **249.**
42. Stone, H.L.: "Estimation of three-phase relative permeability and residual oil data," *J. Can. Petrol. Technol.* (1973) **12,** No. 4, 53.
43. Lax, P.D.: "Hyperbolic systems of conservation laws, II," *Comm. Pure Appl. Math.* (1957) **10,** 537.
44. Liu, T.-P.: "The Riemann problem for general 2×2 conservation laws," *Trans. Amer. Math. Soc.* (1974) **199,** 89.
45. Liu, T.-P.: "The Riemann problem for general systems of conservation laws," *J. Differential Equations* (1975) **18,** 218.
46. Dafermos, C.M.: *Hyperbolic Conservation Laws in Continuum Physics,* Springer-Verlag, Berlin (2000).
47. Ancona, F. and Marson, A.: "A note on the Riemann problem for general *n*×*n* conservation laws," *J. Math. Anal. Appl.* (2001) **260,** 279.
48. Juanes, R. and Patzek, T.W.: "Analytical solution to the Riemann problem of three-phase flow in porous media," *Transp. Porous Media* (2004) **55,** No. 1, 47.
49. Kyte, J.R., Stanclift, R.J. Jr., Stephan, S.C. Jr., and Rapoport, L.A.: "Mechanism of Waterflooding in the Presence of Free Gas," *Trans.,* AIME (1956) 215, **207.**
50. Willhite, G.P.: *Waterflooding,* Society of Petroleum Engineers, Richardson, Texas (1986).
51. Juanes, R. and Patzek, T.W.: "Relative Permeabilities in Co-Current Three-Phase Displacements With Gravity," paper SPE 83445 presented at the SPE Western Regional/AAPG Pacific Section Joint Meeting, Long Beach, California, 19–24 May.
52. Juanes, R., Lie, K.-A., and Kippe, V.: "A front-tracking method for hyperbolic three-phase models," *Proc.,* 2004 European Conference on the Mathematics of Oil Recovery, Cannes, France.
53. Lie, K.-A. and Juanes, R.: "A front-tracking method for the simulation of three-phase flow in porous media," *Comput. Geos.* (2004) (submitted).

Ruben Juanes is an acting assistant professor in the Dept. of Petroleum Engineering at Stanford U. e-mail: ruben.juanes@stanford.edu. Before coming to the United States, he was an assistant professor in the Dept. of Mathematical Methods at the U. of La Coruña, Spain. He has authored or coauthored more than 25 papers on mathematical and numerical modeling of flow in porous media. His current research interests include the simulation of coupled reservoir geomechanics and fluid flow, multiscale numerical methods, and three-phase flow theory. Juanes holds MS and PhD degrees in civil and environmental engineering from the U. of California at Berkeley. **Tad W. Patzek** is a professor of geoengineering at the Dept. of Civil and Environmental Engineering, U. of California at Berkeley. e-mail: patzek@patzek.berkeley.edu. Before joining the faculty at Berkeley, he was a senior reservoir engineer at Shell Western E&P Inc. (1989–90) and senior research engineer (1986–89) and research engineer (1983–86) at the Enhanced Recovery Research Dept., Shell Development. He has authored or coauthored more than 100 papers and more than 20 expert-witness reports and depositions. His research combines analytical and numerical modeling of earth flow systems with measurement, parameter estimation, and control of these systems. He holds MS and PhD degrees in chemical engineering from the Silesian Technical U., Gliwice, Poland. In 1995, he was a Distinguished Lecturer for SPE.